AD-A080 942 NAVAL POSTGRADUATE SCHOOL MONTEREY CA F/G 20/5
DESIGN CONSIDERATIONS OF A FLOW SYSTEM FOR TRANSIENT LASER DISC--ETC(U)
AUG 79 J STRICKER
UNCLASSIFIED NPS67-79-008 NL

1 OF 1
AD
A080942

END
DATE
FILMED
3-80
DDC

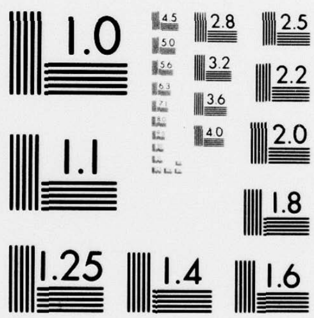
1.0
1.1
1.25
1.4
1.6
1.8
2.0
2.2
2.5
2.8
3.2
3.6
4.0

NAVAL POSTGRADUATE SCHOOL

Monterey, California

DESIGN CONSIDERATIONS OF A FLOW SYSTEM
FOR TRANSIENT LASER DISCHARGE EXPERIMENTS

Josef Stricker

August 1979

Approved for public release; distribution unlimited

Prepared for:
Chief of Naval Research
Arlington, VA 22217

NAVAL POSTGRADUATE SCHOOL

Monterey, California

Rear Admiral T. F. Dedman
Superintendent

Jack Borsting
Provost

The work reported herein was supported by the Foundation Research Program of the Naval Postgraduate School with funds provided by the office Chief of Naval Research.

Professor Oscar Biblarz collaborated closely with the author in the preparation of this report.

This report was prepared by:

J. Stricker

Josef Stricker
Adjunct Research Professor
of Department of Aeronautics

Reviewed by:

M. F. Platzer

M. F. Platzer, Chairman
Department of Aeronautics

Released by:

William M. Tolles

W. M. Tolles
Dean of Research

UNCLASSIFIED

SECURITY CLASSIFICATION OF THIS PAGE (When Data Entered)

REPORT DOCUMENTATION PAGE

READ INSTRUCTIONS BEFORE COMPLETING FORM

1. REPORT NUMBER: NPS-67-79-008	2. GOVT ACCESSION NO.
3. RECIPIENT'S CATALOG NUMBER	
4. TITLE (and Subtitle): DESIGN CONSIDERATIONS OF A FLOW SYSTEM FOR TRANSIENT LASER DISCHARGE EXPERIMENTS	5. TYPE OF REPORT & PERIOD COVERED: 1 August – 15 October
	6. PERFORMING ORG. REPORT NUMBER
7. AUTHOR(s): JOSEF STRICKER	8. CONTRACT OR GRANT NUMBER(s)
9. PERFORMING ORGANIZATION NAME AND ADDRESS: NAVAL POSTGRADUATE SCHOOL, Monterey, CA 93940	10. PROGRAM ELEMENT, PROJECT, TASK AREA & WORK UNIT NUMBERS: 61152N, RR 000-01-01, N0001479WR90027
11. CONTROLLING OFFICE NAME AND ADDRESS: NAVAL POSTGRADUATE SCHOOL, Monterey, CA 93940	12. REPORT DATE: August 1979
	13. NUMBER OF PAGES: 31
14. MONITORING AGENCY NAME & ADDRESS (if different from Controlling Office)	15. SECURITY CLASS. (of this report): Unclassified
	15a. DECLASSIFICATION/DOWNGRADING SCHEDULE

16. DISTRIBUTION STATEMENT (of this Report)

Approved for Public Release; Distribution unlimited

17. DISTRIBUTION STATEMENT (of the abstract entered in Block 20, if different from Report)

18. SUPPLEMENTARY NOTES

Electrical Discharges
Gasdynamics
Electrical lasers
Ludwieg tubes

19. KEY WORDS (Continue on reverse side if necessary and identify by block number)

20. ABSTRACT (Continue on reverse side if necessary and identify by block number)

This report examines design considerations of a flow system for transient electrical laser experiments. After a brief review of corona discharge gas flow interaction phenomena, the choice of the size and operating conditions of the discharge cell are discussed. Once those parameters are established, the flow system, which consists essentially of a Ludwieg tube, is designed. Attention is paid to flow starting times, to the available time of steady state flow, and to the effects of the boundary layer on the core flow. Suggested experiments and instrumentation are given as well in this report.

DD FORM 1473, 1 JAN 73 — EDITION OF 1 NOV 65 IS OBSOLETE
S/N 0102-014-6601

UNCLASSIFIED

SECURITY CLASSIFICATION OF THIS PAGE (When Data Entered)

TABLE OF CONTENTS

LIST OF FIGURES

Abstract

This report examines design considerations of a flow system for transient electrical laser experiments. After a brief review of corona discharge gas flow interaction phenomena, the choice of the size and operating conditions of the discharge cell are discussed. Once those parameters are established, the flow system, which consists essentially of a Ludwieg tube, is designed. Attention is paid to flow starting times, to the available time of steady state flow, and to the effects of the boundary layer on the core flow. Suggested experiments and instrumentation are given, as well, in this report.

I. INTRODUCTION

The effect of gasdynamic means for stabilizing corona discharges in atmospheric air has been shown[1,2,3] to be significantly important. By choosing the right turbulence spectrum and flow speed, the electrical power fed into a diffuse corona discharge has been improved by as much as 500 times above the maximum no-flow power. The influence of turbulence, which is more substantial at the higher pressures (~1 atm), is to promote better mixing and homogeneity of the gas. Thus, by gasdynamic means, molecular gases are able to accept higher diffuse discharge power, making such discharge attractive for electric gas laser operation because of the promise of attractive output power capabilities.

The temporal nonuniformities of the gas density created by the turbulence may cause phase distortions in the laser output beam, and thus deteriorate the laser performance, (due to the effect of the phase distortions on the far field intensity distribution). However, turbulent corona discharge studies show that the strongly decaying turbulence mainly affects the discharge at the region close to anode tips[2,4] where the electric field is strong and the plasma is formed; this is the corona region of length L_a, and has a strong nonuniform electric field E_a (Fig. 1). The external zone is a quasi-neutral zone which has a length of L_b, $L_b >> L_a$, and an electric field E_b which is considerably lower and more uniform than E_a. Thus, by exciting the turbulence at the anode tips region and letting the turbulence decay and become very weak at the external zone, where laser action occurs, the density nonuniformity problem can be reduced to minimum.

The separation of the discharge region into two main regions with space scales L_a and L_b (where $L_a \ll L_b$) and electric fields E_a and E_b (where $E_a \gg E_b$) appears to be very useful for efficient laser operation. Those regions may be controlled, almost independently, by changing electrode geometry (anode tips radii, electrode separation, electrode material, etc.) and flow characteristics. It is possible to choose the average electric field in the external region so that the E/N value will be in such a range that most of the electron energy will go to excite the upper laser level; as for example, in a CO_2 laser containing a mixture of $He/N_2/CO_2$ in a volumetric ratio of 3/2/1, more than 80% of the electron energy goes into the $CO_2(001)$ and $N_2(v=1)$ vibrational levels for the value of $E/N \simeq 2 \times 10^{-16}\ Vcm^2$ (5,6). In this respect, an analogy can be made between a c.w. electron-beam-sustained electric discharge and a c.w. gasdynamic stabilized corona discharge; both cases operate in the Ionizer/Sustainer mode(7), which means that there is a separation between the electric field that produces the electrons and the sustained discharge, where the electrons acquire their optimal temperature Te (Te is determined by E/N) for laser action.

In this report we propose an experimental study of the effects of gasdynamic means (mainly turbulence and flow speed) and different geometrical parameters of the electrodes on corona discharges for laser applications.

The experimental system proposed is a versatile inexpensive set-up, in which the following can be studied.

Fluid dynamics measurements:

Turbulence spectrum	Flow rates	Temperatures
Velocity profiles	Pressures	

Electrical measurements:

V-I characteristics

probes for E, Ne, and T_e measurements

Optical measurements:

Photography

Schlieren photography

Interferograms

Light emission spectroscopy

Laser performance measurements:

Small signal gain

Output power measurements

Parameters to be studied:

Turbulence intensity and spectrum

Flow rates (speed and pressure)

Gas mixtures

Discharge electrical energy

Distance between electrodes

Electrodes geometry

Preionizing devices, like u.v. radiation

To generate the flow through the corona discharge, the application of the Ludwieg tube[8] principle has been considered to be an attractive proposition because of its simplicity, low cost and also high flow quality. The useful flow time of this device depends mainly on the charge tube length and on the speed of sound of the gas in the tube (see Section III). For air this time is approximately 5 $\frac{\text{msec}}{\text{meter length}}$. For a charge tube of the order of 4m in length, the net useful flow time will be 15-20 msec, which corresponds to ~30 cavity flow times (for 5 cm cavity length and gas speed of 100 m/sec). This procedure effectively simulates cw operation without requiring the heat sink electrodes, large compressors, heat exchanger etc., that would be necessary for true c.w. operation. All other relevant characteristic times are much shorter than the flow time[2].

Section II deals with the basic design and sizing of the test cell. Once the cell dimensions, the pressure of the gas and its flow speed are determined, the Ludwieg tube flow system can be designed. The detailed considerations of the design are given in Section III. The overall experimental set-up is shown schematically in Fig. 2.

II. TEST CELL DESIGN

The test section design is basically the same as that of the cell used previously in the gasdynamic-discharge interaction studies[2,3]. Some changes have to be made due to the use of this cell for laser experiments and as being a part of a different flow system.

1. Cell Operating Conditions

Gas mixtures Different gas mixtures are going to be used in this system: N_2, He, CO_2, CO ... etc. As far as a flow system design is concerned, the difference among those mixtures is their specific heat ratio γ and molecular weight.

will consider two values for γ:

$\gamma = 1.4$ (diatomic molecular gas)

$\gamma = 1.67$ (monatomic gas)

Gas pressure The cell will be operated at pressures around 500 torr which is the pressure at which maximum electrical power can be dumped into the corona discharge in no flowing air with 4cm electrode gap[3]. For different gases, different electrode gaps and for flowing gases the optimum operating pressure varies, thus the system will be designed to operate in the pressure range of $200 \leq p \leq 800$ Torr (lower and higher pressures can be achieved as well).

Flow speed The gasdynamics-discharge interaction becomes effective at flow speeds of ~100 m/sec[3]. The faster the flow is, the more discharge performance improves. The cell will be designed to have a flow of about Mach number $M = 0.5$.

2. Cell dimensions

Cross section dimensions:

Cell height: d = 2.22", 5.5 cm .

Cell width: b = 6.5" , 16 cm .

Dimension along the flow direction:

Cell length: c = 4" , 10 cm .

Dimensions d and c are the same as those in Ref. 3; however, the cell width, b, is bigger since along this direction the small signal gain (s.s.g.) is measured and laser cavity will be aligned. The s.s.g. reported in the literature[6,9] for electrical lasers, range from 1% to 4% cm^{-1}; 16 cm cavity length should be adequate for gain and power measurements.

3. Nozzle throat

The cross section area of the discharge cell is $S = b \times d = 88\ cm^2$. In order to obtain $M = 0.5$ in the test section, the cross section area A^*, at the throat for the different values of γ, are given in Table I:

	$\gamma = 1.4$	$\gamma = 1.67$
A/A^*	1.34	1.31
$A^*(cm^2)$	66	67
$h^*(cm)$	4.1	4.2

Table I

Table I give also the values of throat height h^*, for a one dimensional nozzle.

Turbulence generating plates have to be inserted ahead of the electrode tips. Since the effective cross section of those plates is smaller than that of the cell, their effective cross section should exceed the values of A* given in Table I; otherwise, the flow will choke at the plate, prior to reaching the test section.

The turbulent plate used in previous experiments had an area blockage of the order of 50%, which is much above the 34% allowed for this design. A new design and location of those plates have to be considered. One way of improving the plate blockage is to mount the turbulence generators closer to the electrode tips. This will enable a weaker turbulence generation (thus, a smaller blockage) since the decay of the turbulence at the electrode tips will be insignificantly small. One way of doing it is shown in Fig. 3.

4. Electrical power heat addition

The effect of adding heat to a compressible flow is to send compression waves into the flow which change flow parameters; heat addition to subsonic flow will accelerate the flow and for a critical value of heat, q_{cr}, the flow will be choked.[10]

$$Q_{cr} = \frac{q_{cr}}{C_p T_{stag}} = \frac{1}{2(\gamma + 1)M^2} \frac{(1 + \gamma M^2)^2}{1 + \frac{\gamma - 1}{2} M^2} - 1$$

Typical mass flow rates through the cell:

$$\dot{m} = \rho A v = \frac{P}{(R/M)T} Av$$

for N_2: $$\dot{m} = \frac{\frac{10^6}{2} \times 88 \times 2 \times 10^4}{\left(\frac{8.3 \times 10^7}{28}\right) \times 300} \simeq 1 \text{ Kg/sec}$$

for H_e: $$\dot{m} = \frac{\frac{10^6}{2} \times 88 \times 2 \times 10^4}{\left(\frac{8.3 \times 10^7}{4}\right) \times 300} \simeq 0.14 \text{ Kg/sec}$$

Typical critical heat addition values are given in Table II:

	Q_{cr}	q_{cr} kw/kg/sec	q_{cr}, kw, For typical $\dot{m}$ values
for N_2	0.45	140	140
for H_e	0.4	620	87

Table II

The power supply available has ~1 kw power output which is very low power compared to q_{cr}.

III. LUDWIEG TUBE

1. Introduction

The Ludwieg tube flow system is shown schematically in Figure 2. The Ludwieg tube consists of a long tube, charge tube, where the gas is initially compressed to the desired charge pressure, P_4. A transition section channels the flow from the circular charge tube to the rectangular test section which is a part of a converging-diverging supersonic nozzle. The gas expanding through the nozzle is discharged through a short diffuser into a dump tank. A diaphragm separates the driver and driven sections. The diaphragm can be located either downstream or upstream of the nozzle.

The flow is initiated by the rupture of the diaphragm. In the case of an upstream diaphragm, a backwards facing centered expansion fan propagates into the charge tube. This fan is reflected at the closed end of the tube and returns back to the nozzle. This is called the first flow cycle; a simplified wave diagram is shown in Fig. 4(a). Between the time when the tail of the expansion wave leaves the nozzle entrance and when the head of the reflected fan reaches the nozzle again, the stagnation conditions ahead of the nozzle remain constant and a clean steady flow may be established in the nozzle. A second flow cycle (and others) follows the first one but the stagnation parameters are different. The duration of the steady flow, for a certain gas, is primarily a function of the charge tube length and we are interested to make it as long as possible; there is a limit on the length of the tube set by the growth of the boundary layer[11,12,13]. The boundary-layer growth sets also a limit on the diameter of the tube and on the flow Mach number, M_3, in the charge tube. Subsequent to the diaphragm rupture, a shock wave and a contact surface proceed downstream through the driven section. Additional waves follow the contact surface to adjust the nozzle test section pressure to the freestream pressure corresponding to the designed Mach number expected at the nozzle exit for a given nozzle(14). The steady supersonic flow in the nozzle is not established until all those waves are swept out the nozzle. The time required to get the flow started, that is, the time required to achieve a steady flow from rest, in the supersonic nozzle, is a very important performance criterion. It is important to minimize the start time in order to maximize the duration of the steady state conditions for a fixed charge tube length(14,15).

For downstream diaphragm location, the wave diagram is different from the case where the diaphragm is located upstream, a simplified x - t diagram is shown in Fig. 4(b). As soon as the local sonic velocity is reached at the nozzle throat, no further expansion waves can pass through into the tube and an expansion fan of finite width passes down the tube.

For an upstream diaphragm location, the starting times at the nozzle exit are reported to be shorter than those obtained with the downstream diaphragm location(15). However, the disadvantage of the upstream location diaphragm is that when breaking the diaphragm, particles might tear off and disturb the flow in the test section.

2. Charge tube diameter and length

Economic considerations dictate that a minimum charge tube diameter be used for a given test section size. This results in a relatively small contraction (small ratio between nozzle throat area to charge tube area) which requires high Mach number, M_3, at the charge tube. This will cause the boundary layer to have a dominant effect on nozzle flow.

It is suggested to have the I.D. of the charge tube to be the same as the dimension b of the test cell, i.e. 16 cm. In this case A_4/A^* and M_3 are given in Table III.

	$\gamma = 1.4$	$\gamma = 1.67$
A_4/A^*	3.05	3.00
M_3	0.2	0.19

Table III

If a tube with a larger diameter is available (like 20cm), it will improve the performance of the system, since M_3 will be smaller. It is not recommended to use a plenum chamber upstream of the nozzle inlet (to slow and mix the core and boundary layer flows emerging from the pipe) since it will be shown that for $M_3 \approx 0.2$ the disturbances introduced by the boundary layer growth are small while the starting time is going to be much longer by introducing the plenum chamber.

δ^*/d is given as a function of instantaneous aspect ratio of the flow s/d, P_4d and M_3, in the form of $\delta^*/d \dfrac{(P_4 d)^{1/5}}{(s/d)^{4/5}}$ by Russel[11], based on Becker's model for δ^*/d[16], where δ^* is the boundary layer displacement thickness, at a distance s from the expansion wave head, and d is the charge tube diameter.

$$\text{for } M_3 = 0.2 \quad \frac{\delta^*}{d} \frac{(P_4 d)^{1/5}}{(s/d)^{4/5}} = 5 \times 10^{-4} \text{ (atm - m)}^{1/5}$$

At the end of the test time, $s = 2L$ and the thickness of the boundary layer is $\delta \approx 10\delta^*$. For $P_4 = 1$ atm, L = 3 m and d = 0.16 m, we get $\delta^*/d = 1.3\%$, $\delta \simeq 0.02$ m and $\delta/d \simeq 13\%$.

The perturbations in the core flow due to the boundary layer, when the test period is over, are (for the same parameters used for $\frac{\delta^*}{d}$ calculations):

$$-\frac{\Delta P_3}{P_3} \frac{(P_4 d)^{1/5}}{(L/d)^{4/5}} = 4.3 \times 10^{-4} \Rightarrow -\frac{\Delta P_3}{P_3} = 6.5 \times 10^{-3}$$

$$\frac{\Delta v_3}{v_3} \frac{(P_4 d)^{1/5}}{(L/d)^{4/5}} = 3.2 \times 10^{-3} \Rightarrow \frac{\Delta v_3}{v_3} = 4.8 \times 10^{-2}$$

$$\frac{\Delta T_3}{T_3} = \frac{\gamma - 1}{\gamma} \frac{\Delta P_3}{P_3} = -\frac{0.4}{1.4} \times 6.5 \times 10^{-3} = -1.7 \times 10^{-3}$$

which are relatively very small disturbances.

The effects of the above described core perturbations on the downstream flow were discussed by Russell[11]. He evaluated the boundary layer along the walls of a set of specified nozzles, The results for different values of δ^*/d, M_3 and M (Mach number in the nozzle) are presented in Fig. 7 of his paper; he presents the effective area - $\frac{(A/A^*)_{eff} - A/A^*}{A/A^*}$ as a function of δ^*/d for different values of M_3 and M, where $(A/A^*)_{eff}$ is the test section - to - throat area ratio with boundary-layer correction.

A/A^* is the geometric area ratio, with no corrections.

For the value of $P_4 d = 0.5$ atm-m, Russell found that with $10^{-4} \leq \delta^*/d \leq 1\%$, the effective area change parameter has a finite value determined by the normal steady boundary layer correction of the nozzle itself (in our case $P_o d \approx 2 \times 0.16 \simeq 0.3$. There is a weak dependence on pressure level $(P_4 d)^{-1/5}$).

To summarize:

for M = 0.5 Mach number flow in the test section, d=16cm, L=3m and $M_3 = 0.2$

$$\delta^*/d = 1.3\%, \ \delta/d = 13\%$$

$$\frac{\Delta P_3}{P_3} = 0.6\%, \ \Delta V_3/V_3 = 4\%$$

$$\frac{(A/A^*)_{eff} - A/A^*}{A/A^*} \simeq 0$$ (contribution from charge tube boundary layer)

3. Test time

The test time, (the time taken for the head of the reflected expansion wave to reach back the throat) for small values of M_3 is given approximately by $2L/a_4$, where a_4 is the sound speed of the undisturbed gas in the charge tube.

The time available falls only slightly with increasing the Mach number M_3 (17).

$$t/t_o = \frac{2}{1 + M_3} \{1 + \frac{\gamma - 1}{2} M_3\}^{\frac{\gamma + 1}{2(\gamma - 1)}},$$

where $t_o = L/a_4$. For $M_3 = 0.2$ and L = 3m, the calculated values of t_o and t are given in Table IV.

	$\gamma = 1.4$	$\gamma = 1.67$
a_4 (m/sec)	350	1000
t_o (msec)	8.55	3
t/t_o	1.88	1.9
t (msec)	16	5.7

Table IV

4. Starting times

The starting time of supersonic flow at a given location in the flow system is defined as the time elapsed between the arrival of the head of the expansion fan (downstream diaphragm), or shock wave (upstream diaphragm) and the instance where the pressure becomes time independent, i.e., when steady flow is established. For an upstream diaphragm location, the starting times at the nozzle exit are reported to be shorter than those obtained with the downstream diaphragm location[15]

a. Downstream diaphragm location:

According to ref. 15, (they used a Ludwieg Tube with a charge tube tube of 670 cm in length and I.D. of 13.4 cm) the starting times at the nozzle exit are independent of the initial downstream pressure p_1, except in the range above performance limit. Starting times increase with diffuser length. The starting times upstream of the nozzle throat do not depend noticeably on diffuser length, and are of the order of 0.5 msec, where the starting times in the diverging part of the nozzle are of the order of 6 msec. The experimental results are presented in dimensionless starting time t_s/τ_f as a function of dimensionless axial distance x/D, where τ_f is defined as ℓ/a^*; $\ell = \sqrt{R^*h^*}$, R^* is the radius of curvature at the nozzle throat, h^* the nozzle height and a^* the speed of sound at the throat. At the subsonic nozzle section $t_s/\tau_f \simeq 3$ and at the nozzle exit $t_s/\tau_f \simeq 40$. In our case, the starting time in the subsonic section will be $t_s \simeq 1$ msec and in the supersonic section $t_s \simeq 8$ msec, for N_2. For other gases, the starting time scales inversely to a^*.

b. Upstream diaphragm location

The starting times, at the exit of the nozzle, increase with initial downstream pressure, P_1, and increase also with diffuser length. The starting times are of the order of 2 msec at nozzle exit and P_4/P_1 should be at least of the order of 10 in order to start the flow[15].

Summary:

It is recommended to use the downstream diaphragm location, mainly because the starting time in the subsonic portion of the nozzle is very short ($\sim$ 1 msec) and the troubles of having diaphragm particles in the flow are eliminated. For supersonic experiments, it might be an advantage to have the diaphragm located upstream. The diaphragm holder unit can be designed so that there will be a possibility to mount it either downstream or upstream.

4. Charge tube pressures and temperatures

The pressures and temperatures, P_4 and T_4, in the charge tube, prior to diaphragm rupture, as a function of pressure P_2 and temperature T_2, respectively, where the Mach number of the flow is M_2, is given by[17]:

$$\frac{T_2}{T_4} = \frac{T_{st}}{T_4}\frac{T_2}{T_{st}} = (\frac{T_3}{T_4}\frac{T_{st}}{T_3})\frac{T_2}{T_{st}} = \frac{1 + \frac{\gamma - 1}{2} M_3^2}{(1 + \frac{\gamma - 1}{2} M_3)^2} \frac{1}{1 + \frac{\gamma - 1}{2} M_2^2} \quad (1)$$

$$\frac{P_2}{P_4} = (\frac{T_2}{T_4})^{\frac{\gamma}{\gamma - 1}} \quad (2)$$

$$\text{For } \gamma = 1.4,\ M_3 = 0.2 \rightarrow \frac{T_2}{T_4} = 0.93 \frac{1}{1 + \frac{\gamma - 1}{2} M_2^2}$$

$$\text{For } \gamma = 1.67,\ M_3 = 0.2 \rightarrow \frac{T_2}{T_4} = 0.95 \frac{1}{1 + \frac{\gamma - 1}{2} M_2^2}$$

The corresponding values of P_4/P_2 can be calculated from Eq. (2).

P_4 as a function of P_2 for different values of the M_2 is shown in Fig. 5 and Fig. 6 for $\gamma = 1.4$ and $\gamma = 1.67$ respectively. The values of T_2, for $\gamma = 1.4$ and $\gamma = 1.67$ and different values of M_2 are given in Table V assuming $T_4 = 300^{o}k$:

M_2	0	0.5	1	1.5	2
$\gamma = 1.4$	280	266	233	193	155
$\gamma = 1.67$	285	263	213	162	122

Table V

The pressure, P_1, in the part of the system downstream the diaphragm should be of the order of $P_4/100$ (to get best start times without a diffuser); i.e. $P_1 \approx 1$ torr (see Sec. 5).

5. Diffuser, dump tank and valve

The starting times, as discussed before, become longer with longer diffusers, both for downstream and upstream diaphragm locations.

For a fixed charge tube pressure, and back pressure P_1 being increased gradually, the flow at the diffuser end ceases to start for a certain value of P_1 while further increasing P_1, the supersonic flow at the nozzle exit barely starts. Beyond these critical conditions, the flow at the nozzle exit becomes unstable. The limiting experimental downstream pressure radios, P_1/P_4, were measured by Merkli and Abuaf[15], both for upstream and downstream diaphragm locations, as a function of diffuser length L/D.

It was found that $(P_1/P_4)_{cr}$ for diffuser starting is ~0.11 independent on L/D.

$(P_1/P_4)_{cr}$ for nozzle supersonic flow increases with L/D and reaches a maximum at about L/D ≈ 6 where $(P_1/P_4)_{cr} = 0.22$.

That means that within the available time, the pressure in the dump tank should not increase above 0.1 x P_4; this limiting pressure defines the volume of the dump tank.

The rate of pressure rise inside the tank: The continuity dictates that in the dump tank $V_d \frac{\partial \rho_d}{\partial t} + \dot{m}_d = 0$ where V_d is the tank's volume, ρ_d is the density and $\dot{m}_d$ is the total mass flow into the tank. By differentiating the equation of state, $P_d = \rho_d R T_d$, with respect to time and using the continuity equation, we get

$$\frac{\partial P_d}{\partial t} = RT_d \frac{\partial \rho_d}{\partial t} = \frac{RT_d}{V_d} \dot{m}_d$$

$$\dot{m}_d = \dot{m}_3 = \rho_3 A_3 v_3 = \frac{P_3 A_3 M_3 a_3}{RT_3}$$

$$\therefore \quad \Delta P_d = \frac{T_d P_3 A_3 M_3 a_3}{T_3 V_d} \tau$$

Where τ is the available testing time. Since initially $P_d = P_1 <<$ $0.1P_3$ we may write $\Delta P_d = P_d$; from the last equation:

$$V_d = \left(\frac{T_d}{T_3}\right)\left(\frac{P_3}{P_d}\right)A_3 M_3 a_3 \tau \leq 2 \times 10 \times \Pi \times 8^2 \times 0.2 \times 33000 \times 20 \times 10^{-3}$$

$$V_d \approx 5.3 \times 10^5 \ cm^3$$

It is suggested to install a valve upstream the diapragm, as shown in Fig. 3. After each run, before the ruptured diaphragm is taken off, this valve will be closed and the gas in the system will be saved.

A more efficient way of saving gas will be to use a compressor to compress the gas in the dump tank and recirculate it back to the charge tube. The compressor should be vacuum tight. A simple and inexpensive compressor is suggested in Fig. 7.

IV. INSTRUMENTATION

Pressure gauges

0-5 atm. range for measuring P_4 .

0-100 torr
0-760 torr } Pressure gauges for gas mixtures preparation.
0-2 atm

0-100 torr for measuring P_1

For measuring P_2 and P_3 during the experiment itself, after diaphragm is broken, we need piezoelectric pressure transducers with time response of the order of tens microseconds, in the range of 0-2 atm.

Velocity profiles and turbulence spectrum

For transient flow speed and turbulence measurements, a laser-doppler anemometer or a hot-wire anemometer can be used. The available steady flow time, 10-20 msec, might be too short for appropriate averaging the turbulence spectrum, mainly in the low frequency regime. Therefore it will be necessary to run the flow in a continuous mode (with compressed air) for turbulence spectrum measurements. The transient flow fluctuations may not be averageable but their ability to stabilize the discharge may surpass that of steady flow in which case other measurement forms should be sought.

Voltage current measurements; probes

The voltage and current have to be recorded during the experiment. The simplest way of doing it would be by using an oscilloscope.

The probes used for measuring plasma parameters must be provided with automatic bias sweep, so that the characteristics can be accomplished within the flow time.

Lasing diagnostics

A probe laser for s.s.g. measurements.

A fast response detector (microseconds range).

Power meter.

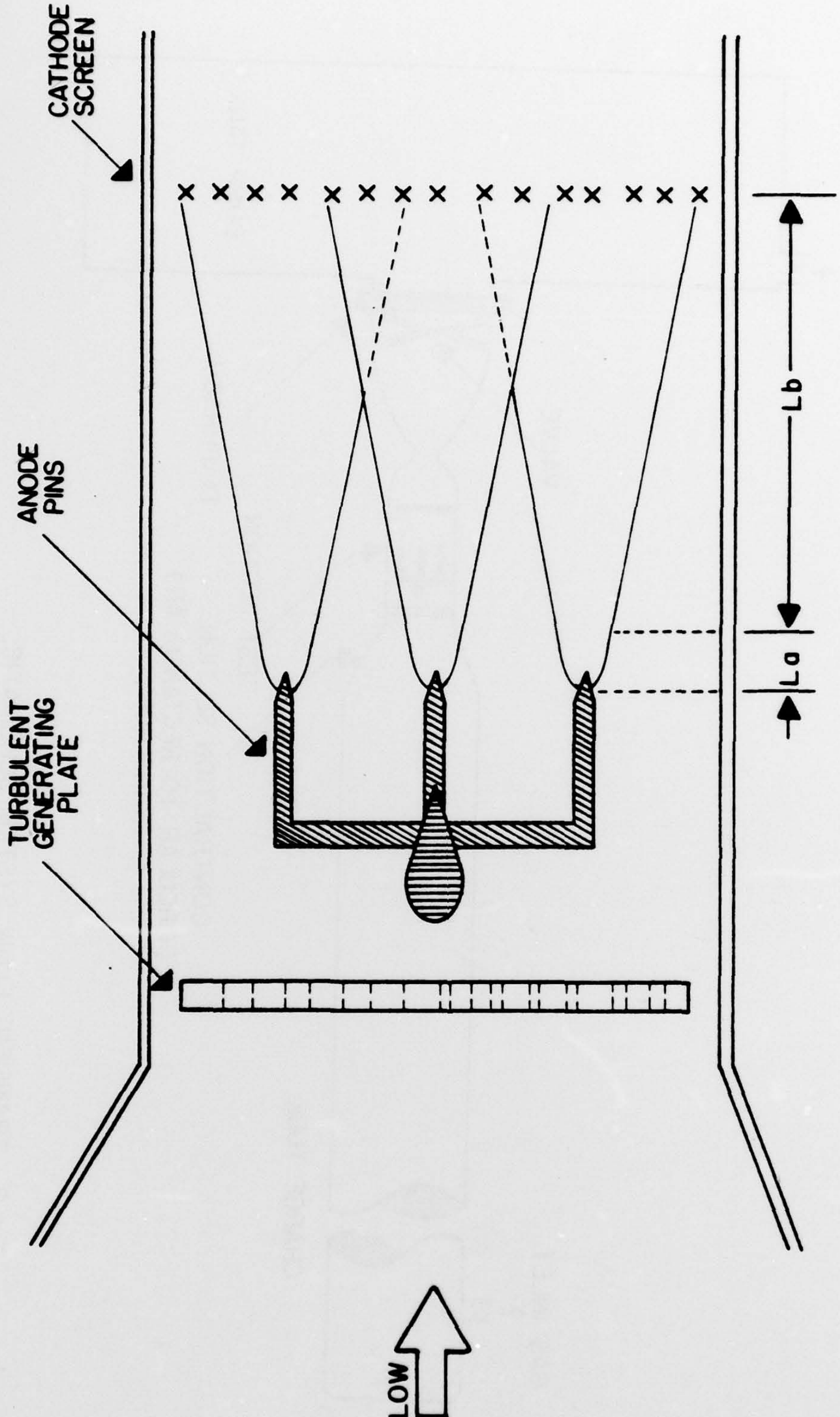

Fig 1. SCHEMATIC OF PRESENT DISCHARGE CELL AND DETAIL OF PIN REGION.

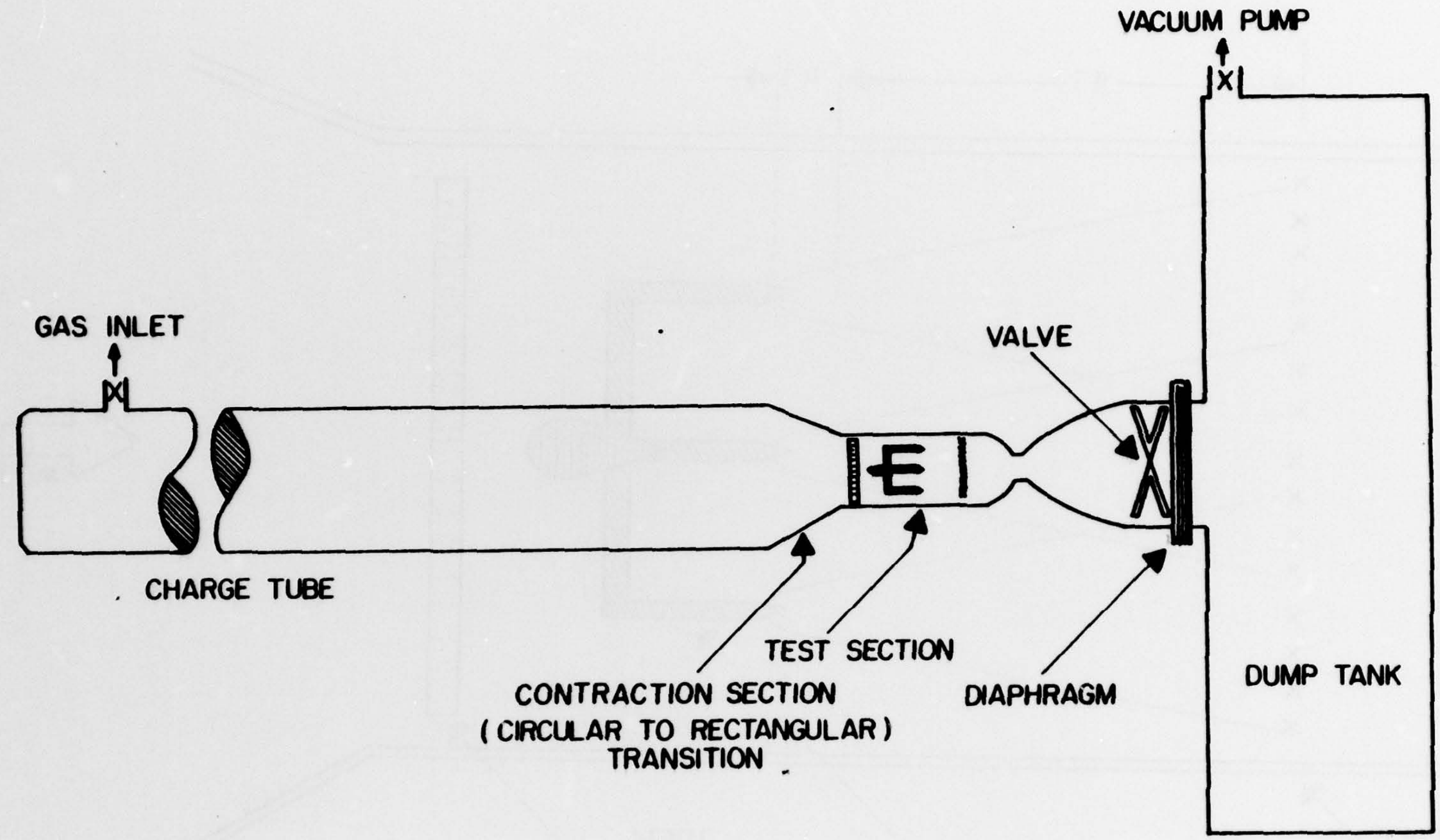

Fig 2. TRANSIENT FLOW SYSTEM SCHEMATIC.

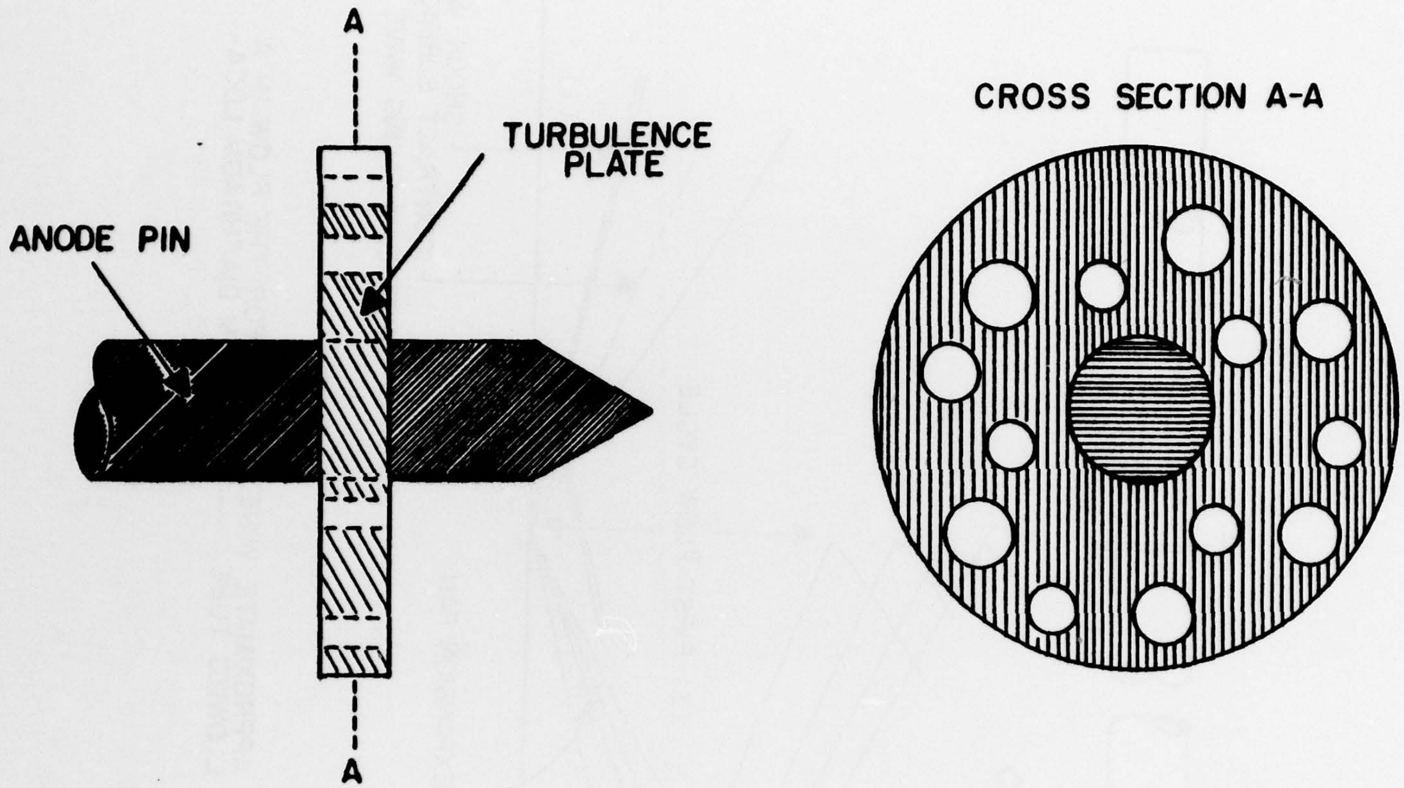

Fig 3. SUGGESTED TURBULENCE GENERATING PLATES MOUNTED CLOSE TO ELECTRODE TIP.

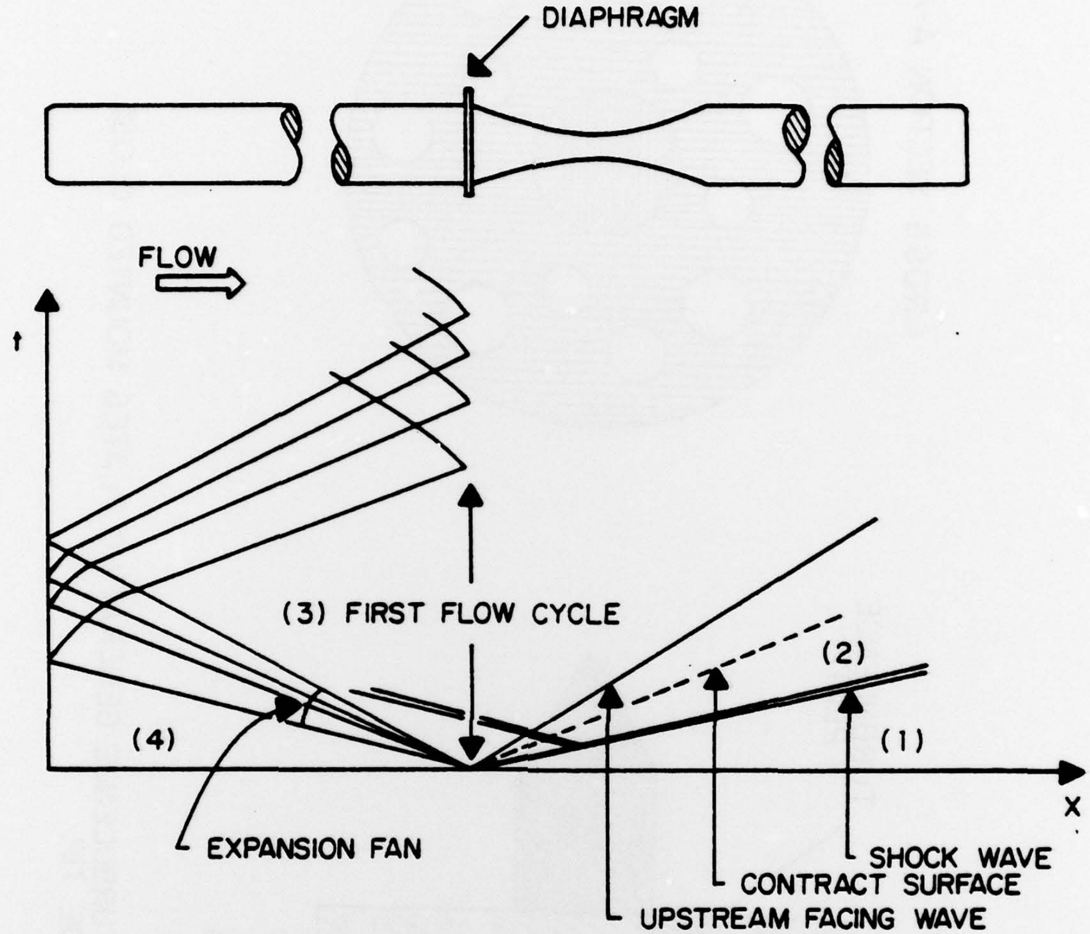

Fig. 4(a) APPROXIMATE WAVE DIAGRAM FOR THE FLOW IN A LUDWIEG TUBE. — UPSTREAM DIAPHRAGM LOCATION.

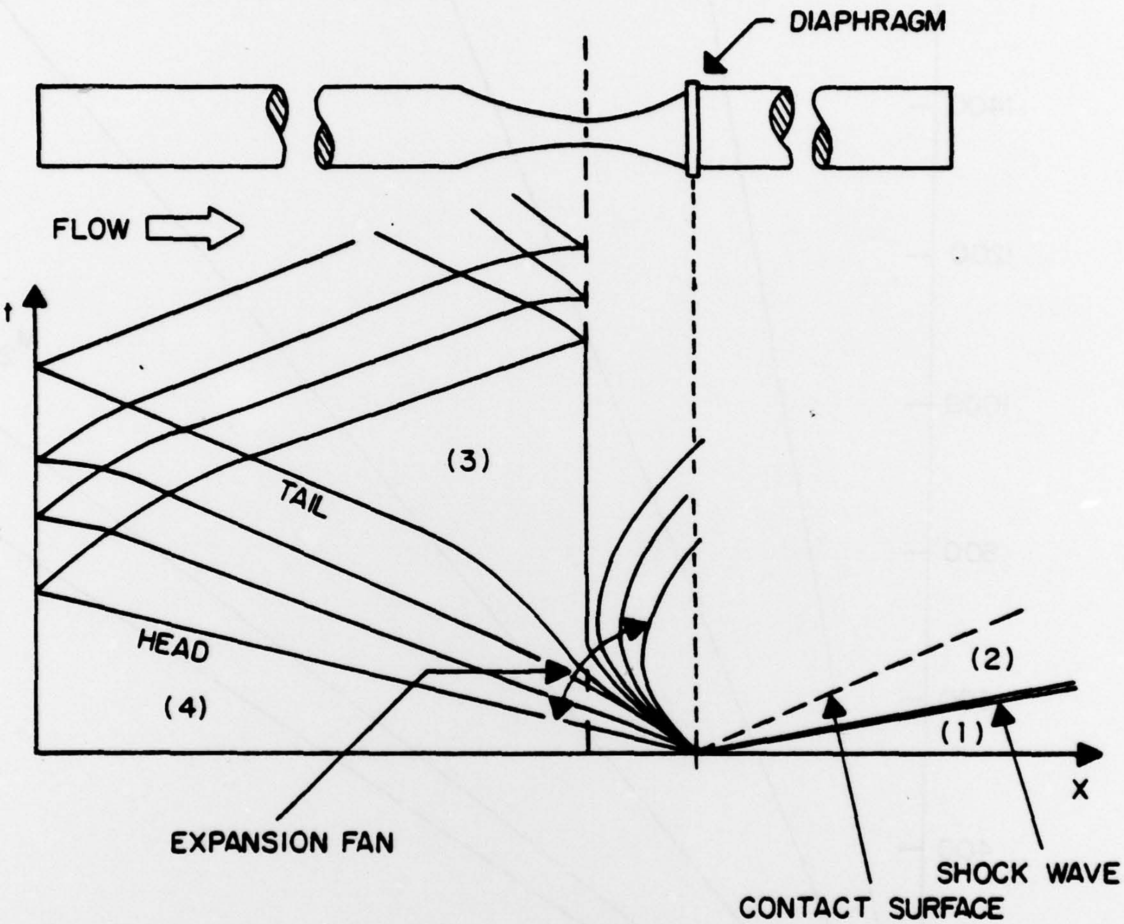

Fig. 4(b) APPROXIMATE WAVE DIAGRAM FOR THE FLOW IN A LUDWIEG TUBE. - DOWNSTREAM DIAPHRAGM LOCATION.

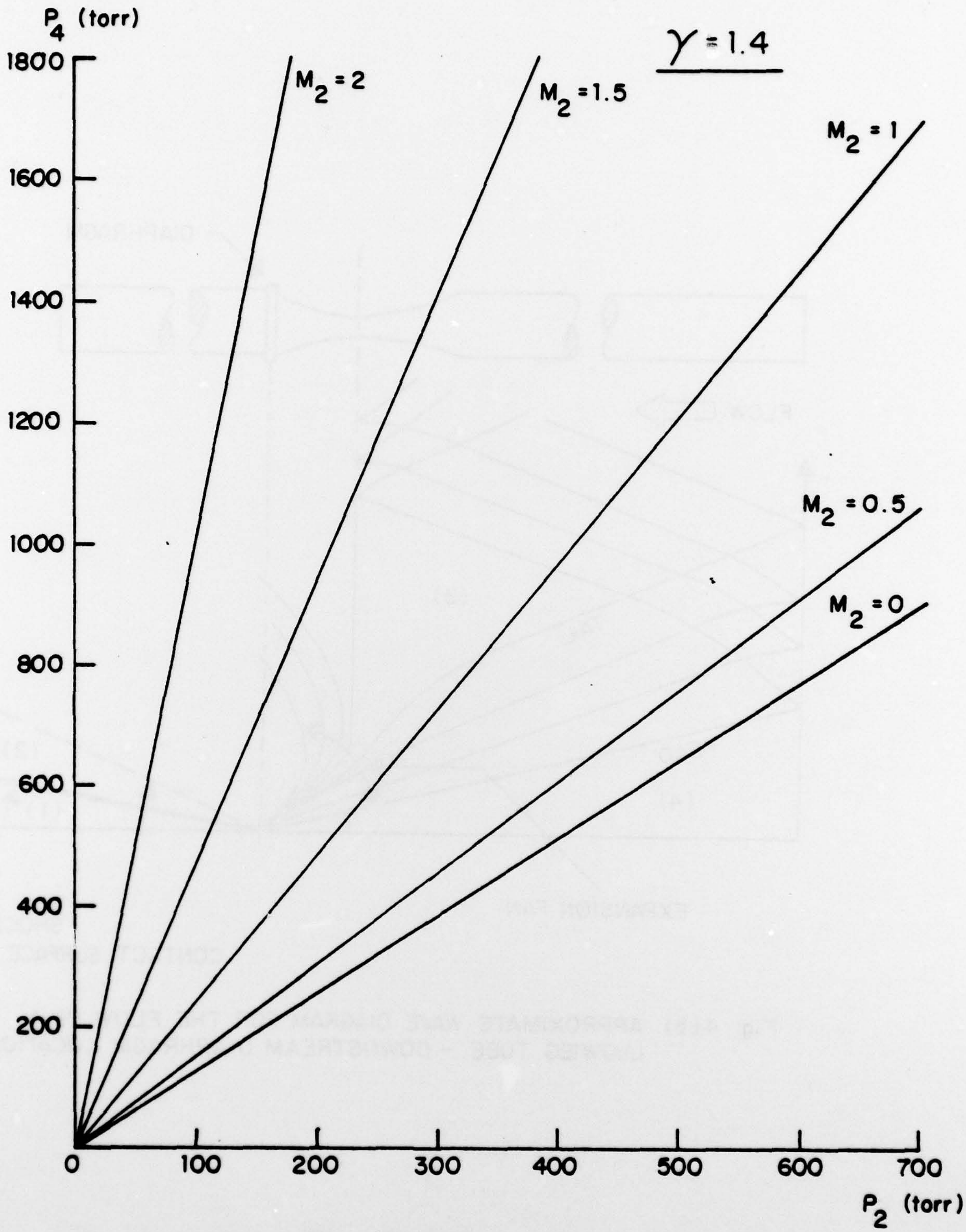

Fig. 5 CHARGE TUBE PRESSURE, P_4, AS A FUNCTION OF CELL PRESSURE, P_2, FOR DIFFERENT VALUES OF M_2. $\gamma = 1.4$

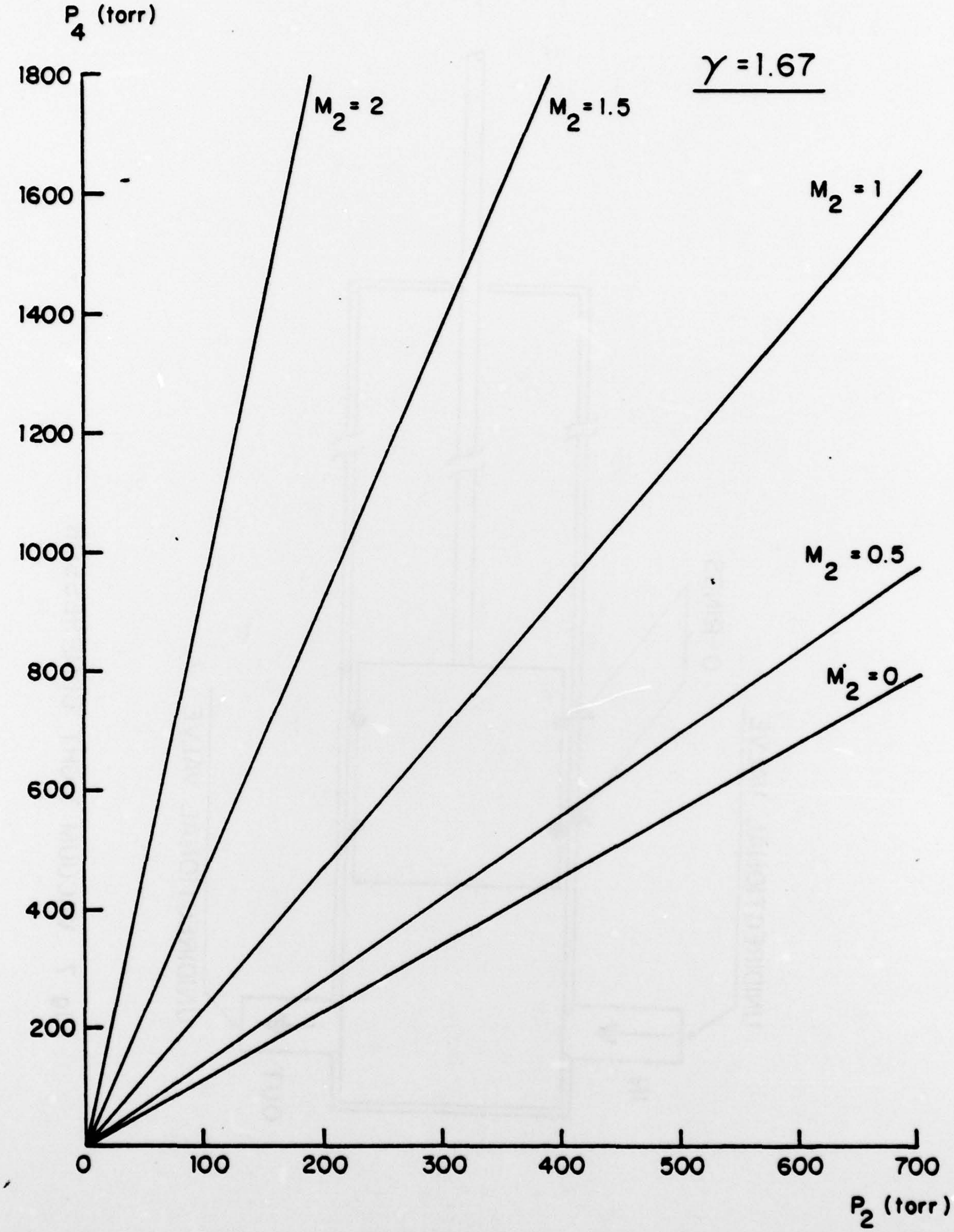

Fig. 6 CHARGE TUBE PRESSURE, P_4, AS A FUNCTION OF CELL PRESSURE, FOR DIFFERENT VALUES OF M_2. $\gamma = 1.67$

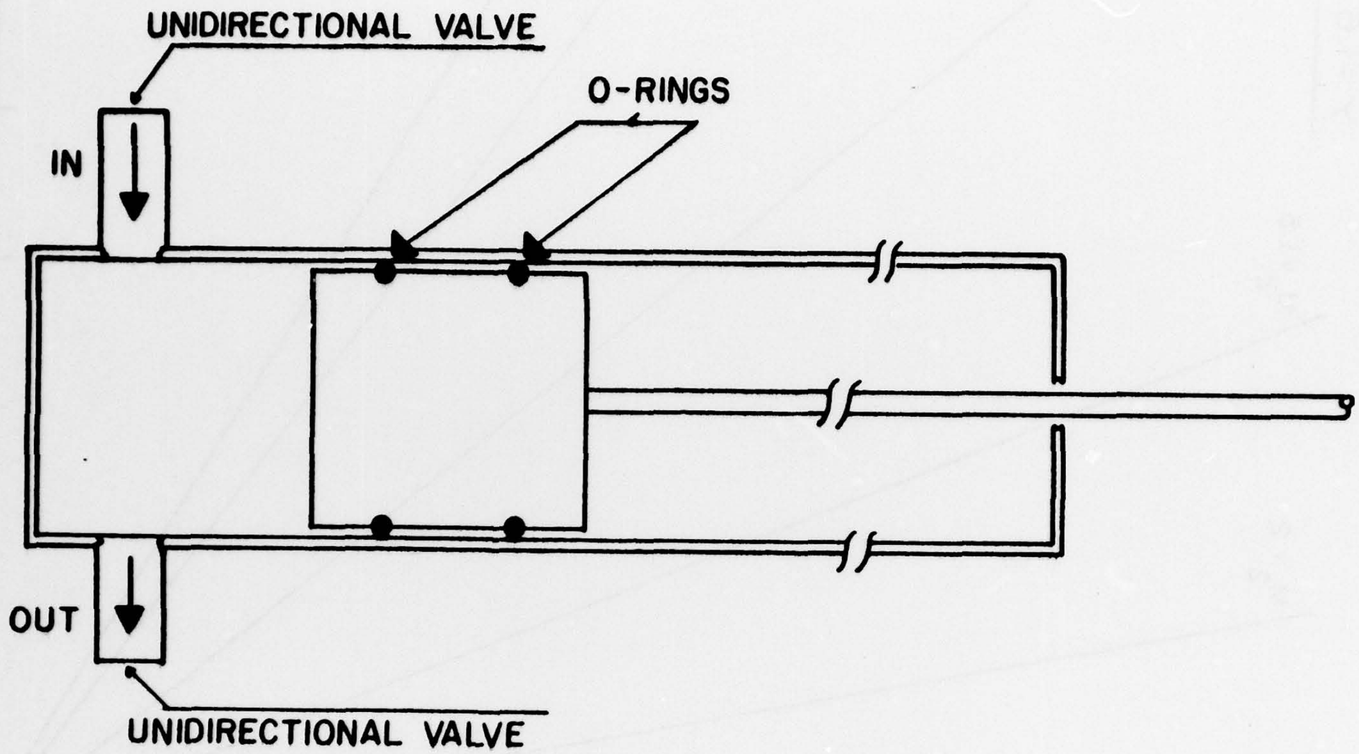

Fig 7. VACUUM TIGHT COMPRESSOR.

LIST OF REFERENCES

1. O. Biblarz and R. E. Nelson, "Turbulence Effects on an Ambient Pressure Discharge," J. Appl. Phys., 45, 633 (1979).

2. O. Biblarz, J. L. Barto and H. A. Post, "Gas Dynamic Effects on Diffuse Electrical Discharge in Air", Israel J. of Tech., 15, 59 (1977).

3. H. A. Post, "Sub-Ambient Controlled Turbulence Effects on Discharge Stabilization for Laser Applications," Master's Thesis, (Sept. 1976) Naval Postgraduate School, Monterey, CA.

4. Y. Khait and O. Biblarz, "Influence of Turbulence on a Diffuse Electrical Gas Discharge Under Moderate Pressures," J. Appl. Phys., 50, 4692, (1979).

5. D. H. Douglas-Hamilton and S. Lowder, "Carbon Monoxide Electric Discharge Laser Kinetics Handbook," AERL Research report: Air Force Weapons Lab. Tech. Report AFWL-TR-74-216 (1974).

6. M. J. Yoder, H. H. Legner, J. H. Jacob and D. R. Ahouse, "Theoretical and Experimental Performance of a High Power CW Electron-Beam-Sustained Electric Laser," J. Appl. Phys., 49, 3171 (1978).

7. I. P. Reilly, "High Power Electric Discharge Lasers," A&A, March 1975, p. 52.

8. H. Ludwieg, "Der Rohrwindkanal," Zeit. fur Flugwissenschaften, 3, 206 (1955).

9. A. K. Levine and A. J. DeMaria, Lasers, Vol. 3, Marcel Dekker, Inc., New York, 1971.

10. J. A. A. John, Gas Dynamics, Allyn and Bacon, Boston, (1976).

11. D. R. Russell and K. O. Tong, "Aerodynamics of High-Performance Ludwieg Tubes," AIAA J., 11, 642, 1973.

12. J. C. Sivells, "Calculation of the Boundary-Layer Growth in a Ludwieg Tube," Arnold Eng. Development Center, Arnold Air Force Base, TN, AEDC-TR-75-118, (Dec. 1975).

13. J. H. Porter and R. F. Starr, "Boundary-Layer Development in the Nozzle and Test Section of a Transonic Ludwieg Tube", AEDC-TR-76-35, (Oct. 76).

14. N. Abuaf, "Straight Duct Supersonic Diffuser Flow in a Ludwieg Tube with Upstream Diaphragm," Dept of Eng. and Appl. Science, Yale University, Scientific Report #6, (Dec. 1976).

15. P. E. Merkli and N. Abuaf., "Flow Starting Times in Constant-Area Supersonic Diffusers," AIAA J., 15, 1718, (1977).

16. E. Becker, "Unsteady Boundary Layer Behind Compression Shocks and Expansion Waves," Progress in Aeronautical Sciences 1, 104, (1973).

17. A. J. Cable and R. N. Cox, "The Ludwieg Pressure-Tube Supersonic Wind Tunnel," The Aeronautical Quarterly, May 1963, p. 144.

DISTRIBUTION LIST

		No. of Copies
1.	Defense Documentation Center Cameron Station Alexandria, Virginia	2
2.	Library Code 0212 Naval Postgraduate School Monterey, California 93940	2
3.	Office of Research Administration Code 012A Naval Postgraduate School Monterey, California 93940	2
4.	Chairman Department of Aeronautics Code 67 Naval Postgraduate School Monterey, California 93940	1
5.	Professor Oscar Biblarz Department of Aeronautics Code 67Bi Naval Postgraduate School Monterey, California 93940	5
6.	Dr. Josef Stricker Department of Aeronautics Technion, Haifa ISRAEL	5
7.	Professor Eli Nissim, Dean Department of Aeronautics Technion, Haifa ISRAEL	1
8.	Dr. Josef Shwartz TRW Room # R1 - 1032 1 Spacepark Redondo Beach, CA 90278	1